SURE 静岡大学学術リポジトリ
Shizuoka University REpository

Dynamics of fast and slow pulse propagation through a microsphere-optical-fiber system

著者	Totsuka Kouki, Tomita Makoto
journal or publication title	Physical Review E
volume	75
number	1
page range	016610-016610
year	2007-01
出版者	American Physical Society
権利	(c)2007 The American Physical Society
URL	http://hdl.handle.net/10297/600

doi: 10.1103/PhysRevE.75.016610

Dynamics of fast and slow pulse propagation through a microsphere–optical-fiber system

Kouki Totsuka and Makoto Tomita
Department of Physics, Faculty of Science, Shizuoka University, 836 Ohya, Surugaku, Shizuoka, 422-8529 Japan
(Received 5 July 2006; published 19 January 2007)

We discuss the mechanism of fast and slow light generation when optical pulses propagate through a fiber taper coupled to an ultrahigh-Q microsphere system in the time domain. Fast and slow light are explained as interference effects between ballistic light through the fiber and circulated light within the sphere. One of the striking effects predicted by this model is dynamic pulse splitting in the transmitted pulse at the critical coupling condition, where the coupling strength between the sphere and fiber equals the round-trip loss in the sphere. By realizing this critical coupling condition experimentally, we observed this dynamic pulse splitting effect.

DOI: 10.1103/PhysRevE.75.016610 PACS number(s): 42.25.Bs, 42.25.Hz, 42.60.Da

The velocity of light is of fundamental interest in physics; fast light has been attracting renewed interest in the context of information velocity and Einstein's special relativity theory, while slow light is discussed in the context of the enhancement of interactions between light and matter. Fast and slow light appear not only in simple absorption or gain lines but also in quantum manipulated atomic systems [1], such as electromagnetically induced transparency and double Raman type resonances [2,3]. Various kinds of nanostructure media, including photonic crystals and resonant photon tunneling systems, have been fabricated, and fast and slow light have been investigated [4–7]. Dielectric microspheres also have potential usefulness in dispersion engineering. These spheres trap light inside and can act as an ultrahigh-Q optical cavity [8,9]. The mode in the spherical cavity is referred to as a whispering gallery mode (WGM), and the resonance linewidth can be reduced to an extremely narrow 10 kHz [10]. Such a narrow resonance strongly modifies the phase of the light, resulting in very steep dispersion, comparable to quantum manipulated atomic systems. This dispersion, associated with the single sphere, as well as periodic arrays of spheres, holds great promise for controlling the propagation velocity of optical pulses [11–18].

In previous papers, we examined pulse propagation in a fiber taper system coupled to a microsphere experimentally [11,12]. It was shown that the dispersion in this system depends strongly on the coupling strength between the sphere and fiber and the round-trip loss within the sphere. In the undercoupling condition, where the coupling is weak compared with the loss, the dispersion shows anomalous behavior and fast light appears. Conversely, in the overcoupling condition, where the coupling strength is strong compared with the loss, normal dispersion is observed, and slow light appears. We observed both fast and slow light within a single microsphere–optical-fiber system by controlling the coupling strength between the sphere and fiber. In this paper, we discuss the mechanisms of fast and slow light generation within the time domain. Fast and slow light are explained as a result of interference effects between ballistic and circulated light within the sphere. The illustration clarifies the processes involved. One of the striking effects predicted in this picture is the dynamic pulse splitting in the transmitted pulse profile at the critical coupling condition, where the coupling strength between the sphere and fiber equals the round-trip loss in the sphere. We realized this critical coupling condition experimentally and observed the dynamic pulse splitting effect.

Figure 1 shows a schematic illustration of the waist region of a microsphere–fiber-taper system. The fiber taper has an air clad structure where the diameter is reduced gradually from normal to several micrometers or even to submicrometer size. The light traveling along the fiber taper is not confined in the glass core, but emerges from the core as a quasiexponentially decaying evanescent wave. When a microsphere is moved into the evanescent wave region, the light traveling though the fiber taper is coupled into the sphere WGM. The light transferred into the WGM is reflected at the sphere boundary by total internal reflection, so that it circulates in orbits near the sphere surface, and is therefore referred to as circulated light. The circulated light also emerges from the sphere surface as an evanescent wave and is coupled back into the fiber taper. Some of the incident light bypasses the sphere and appears directly at the output of the system; this we refer to as ballistic light. Therefore, the total electric field at the output of this system can be described by the sum of the ballistic and circulated light.

When the incident light beam is turned on, the sphere starts to store light energy. The characteristic buildup time is on the order of $1/\delta\omega = Q/\omega$, the inverse of the resonance linewidth. Similarly, when the light beam is turned off, the

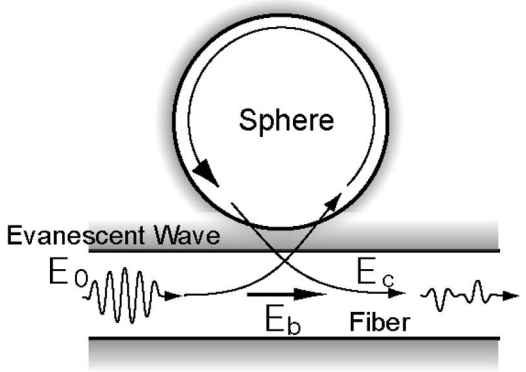

FIG. 1. Schematic illustration of the microsphere-fiber-taper system.

 ©2007 The American Physical Society

light energy leaves the sphere. These buildup and fall-down times create a time delay in the circulated pulse with respect to the ballistic pulse. Both fast and slow light can be described in terms of this delay; more specifically, the ballistic electric field $E_b(\omega)$ and the circulated electric field $E_c(\omega)$ are given, by directional coupling theory [19], as

$$\frac{E_b(\omega)}{E_0(\omega)} = (1-\gamma)^{1/2} y, \tag{1}$$

$$\frac{E_c(\omega)}{E_0(\omega)} = (1-\gamma)^{1/2} \frac{x(1-y^2)\exp[-i\phi(\omega)]}{xy\exp[-i\phi(\omega)]-1} = \sqrt{T_c(\omega)}\exp[-i\theta_c(\omega)],$$

where $E_0(\omega)$ is the electric field of the incident light, $x=(1-\gamma)^{1/2}\exp(-\rho L/2)$ is the loss parameter, $y=\cos(\kappa)$ is the coupling parameter, γ is the insertion loss, ρ is the round-trip loss, κ is the coupling strength between the sphere and the fiber, $\phi(\omega)=n\omega L/c$ with L the round-trip path length of the WGM, $T_c(\omega)$ and $\theta_c(\omega)$ are the intensity and phase shift of the circulated light, respectively, n is the effective refractive index, c is the velocity of light in vacuum, and ω is the frequency of the light. For the modes with low radial indices in a large sphere, we can assume $n=1.458$, i.e., the refractive index of pure silica; and $L=2\pi a$, where a is the radius of the sphere. The phase shift $\theta_c(\omega)$ in the circulated electric field is written as

$$\theta_c(\omega) = \arctan\left\{\frac{-\sin[\phi(\omega)]}{xy-\cos[\phi(\omega)]}\right\}. \tag{2}$$

The transmitted pulse profile of the circulated light is calculated as

$$E_c(t) \propto \int S(\omega)\sqrt{T_c(\omega)}\exp\{-i[\omega t+\theta_c(\omega)+\theta_0]\}d\omega, \tag{3}$$

where $S(\omega)$ is the initial Fourier component of the incident pulse and θ_0 is a constant phase shift relative to the phase shift though the fiber. The total output electric field, $E_{out}(t)$, can be represented by the sum of the two fields, $E_b(t)$ and $E_c(t)$.

Figure 2(a) illustrates the fast light mechanism in the time domain at the resonance frequency for the undercoupling condition schematically. The upper and lower curves show the intensity profiles of the ballistic and circulated light, respectively, calculated at the output of the system. A pulse with a duration of $\Delta t_p=58$ ns and a resonance linewidth of $\delta\omega/2\pi=35$ MHz are assumed. These values correspond to the experimental conditions described below. In Fig. 2(a), the intensity of the circulated light is shown as downward, since at the resonance frequency the phase of the circulated light is shifted by π with respect to the ballistic light. The total output pulses are calculated as the sum of the circulated and ballistic electric fields. It is seen that the temporal profile of the circulated light is delayed 8.4 ns, which is on the order of $1/\delta\omega=Q/\omega$. In the undercoupling condition, the ballistic light is stronger than the circulated light; the tailing part of the ballistic pulse disappears through destructive interference

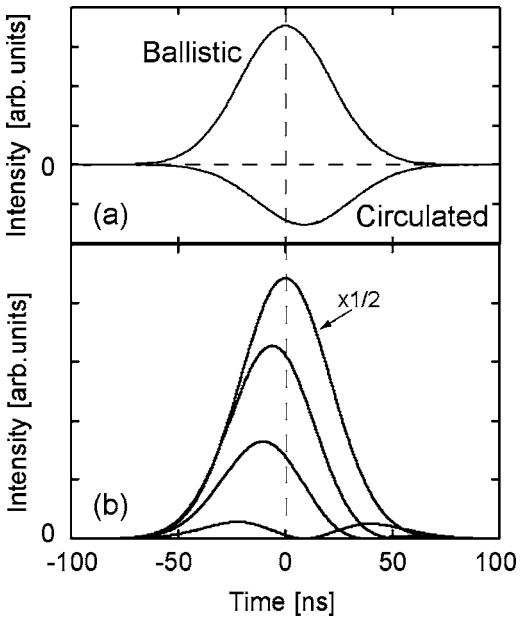

FIG. 2. (a) Illustration of the fast light mechanism in the time domain in the undercoupling condition. The ballistic light is drawn upward, while the circulated light is shown downward, as the phase of the circulated light at the resonance frequency is shifted by π with respect to the ballistic light. These curves are drawn in intensity, but the output pulse is calculated by adding the amplitudes of the two waves. (b) Temporal profile of the output pulse for different parameters of the coupling constant. From top to bottom, $y=1$, 0.99997, 0.99995, and 0.999903, respectively. The magnitude of the curve for $y=1$ is scaled by a factor of 1/2.

with the phase-shifted circulated light. This mechanism makes the pulse profile advanced with respect to the original profile, and explains the fast light in the time domain. Figure 2(b) shows the transmitted pulse profiles for different parameters of y, while the loss parameter x is kept constant at 0.999903. As the coupling strength is increased, the amplitude of the circulated light also increases, but the ballistic light amplitude remains almost unchanged, causing the output pulse to become more advanced. A similar explanation can be made for the overcoupling condition. Figure 3(a) illustrates the slow light mechanism in the time domain. In the overcoupling condition, the circulated light is stronger than the ballistic light. Therefore, the minor field of the ballistic pulse, which is π out of phase to the circulated pulse, cancels the leading edge of the circulated pulse. This mechanism results in a pulse profile delayed with respect to the original profile, and explains slow light in the time domain. Figure 3(b) shows the output pulse profiles for different values of y while $x=0.999903$. Again, as the coupling strength is increased, the circulated light becomes stronger while the ballistic light remains almost unchanged, but here, the delay in the output pulse increases.

We see an analogy between fast and slow light in this sphere system and that in a simple atomic system. Superluminal pulse propagation through an atomic absorption line has been discussed in the time domain [20]. When a coherent pulse propagates through a resonant atomic absorber, more energy is absorbed from the trailing half of the pulse than

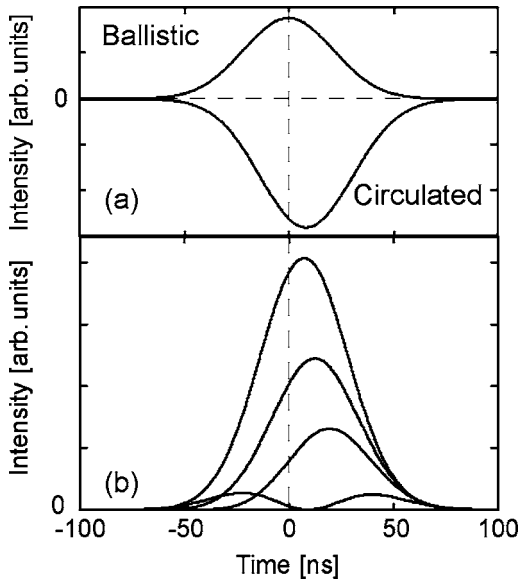

FIG. 3. (a) Illustration of the slow light mechanism in the overcoupling condition. These curves are drawn in intensity, but the output pulse is calculated by adding the amplitudes of the two waves. (b) Temporal profile of the output pulse for different parameters of the coupling parameter y. From bottom to top, $y=0.999903$, 0.9998, 0.9997, and 0.9995, respectively.

from the leading half. This effect results in motion in the pulse position, and the resultant reshaping effect explains the superluminal velocity. In the atomic system, the incident light pulse induces a dipole moment, and this macroscopic dipole radiates back an additional field; in our system, the circulated light generates this field.

The illustration gives a clear understanding of the processes involved with fast and slow light. One of the striking effects predicted by the picture, as discussed above, is dynamic pulse splitting in the transmitted pulses. In steady-state measurements at the critical coupling condition, the transmission becomes zero because the ballistic and circulated light cancel perfectly. In this situation, all the injected energy is dissipated within the sphere. Since the ballistic and circulated pulses are time delayed with respect to each other, their dynamic behavior differs. In the time region, where the two pulses overlap temporally, their intensities cancel. However, the leading edge of the ballistic pulse and the tailing edge of the circulated pulse are not cancelled, and appear at the output. This mechanism produces the dynamic pulse splitting at the critical coupling condition. Note that the total transmission electric field $E_{out}(\omega)$, can also be obtained directly by directional coupling theory, where the group delay time of a wave packet is calculated as $\tau_d=\partial\theta_{total}(\omega)/\partial\omega$, with $\theta_{total}(\omega)$ being the phase shift in the total transmitted field [12]. At the critical coupling condition, however, the phase shift $\theta_{total}(\omega)$ jumps from $\pi/2$ to $-\pi/2$ at the resonance frequency; therefore, $\partial\theta_{total}(\omega)/\partial\omega$ diverges at the resonance frequency and the conventional definition of the group velocity loses physical meaning. This process generating the dynamic pulse splitting is reminiscent of the mechanism of the odd pulse in pulse-shaping optical systems [21]. In generating the odd pulse, an optical pulse is separated into its

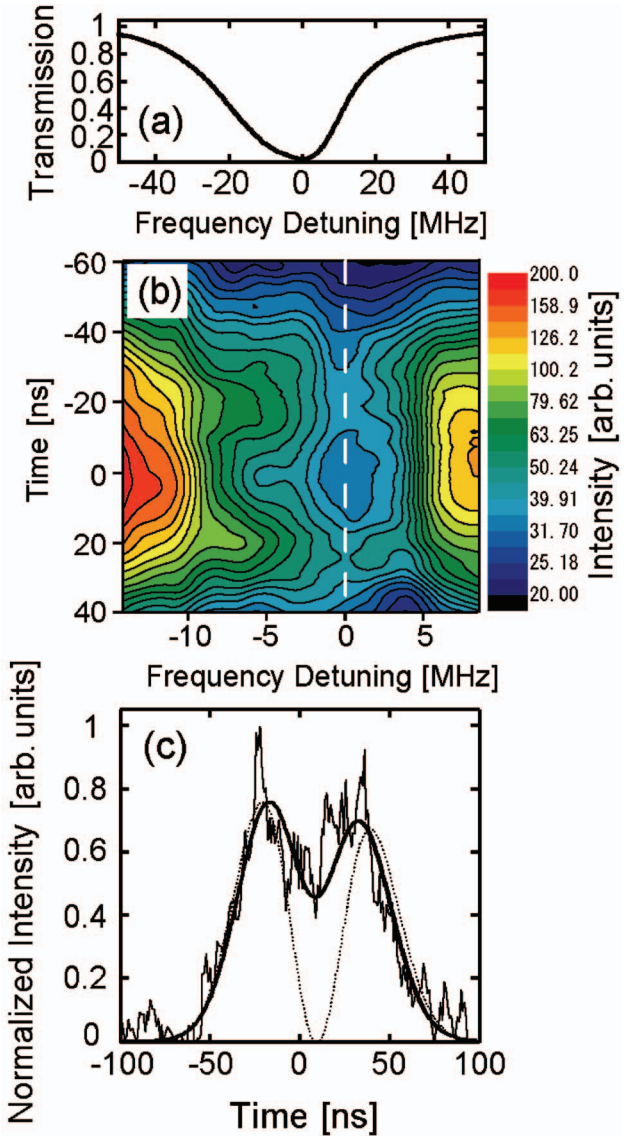

FIG. 4. (Color) (a) The time integrated transmission intensity as a function of the detuning frequency. (b) Two-dimensional contour plot of the transmitted pulse intensity as a function of time and frequency detuning of the laser at the critical coupling condition. The intensity is plotted on a logarithmic scale. The time origin is set at the peak arrival time for a pulse at a far detuning frequency of 100 MHz. (c) The transmitted pulse profile at the resonance frequency along the dashed line in Fig. 4(b). The solid thin curve is the experimental result. The dotted curve is the theoretical pulse profile derived from Eqs. (1) and (2) in the text. The solid thick curve is the calculated profile when 2.9% of the circulated light is assumed to leak into higher modes in the fiber.

spectral components, and then a phase shift of π is added to half of the spectral components. The resultant temporal pulse shape has two peaks when all the spectral components are recombined.

To investigate pulse propagation at the critical coupling condition, we performed an experiment using the sphere-fiber taper system [22]. A silica microsphere was fabricated on the tip of a standard telecommunication optical fiber. To fabricate a sphere smaller than the diameter of the standard

optical fiber, we etched the fiber to 20 μm in diameter using buffered hydrofluoric acid. The end of the etched fiber was fused using a CO_2 laser and a microsphere was self-formed via the surface tension. We used a sphere of radius $a=57.5$ μm for the experiment. The fiber taper was fabricated from the same telecommunication optical fiber. The sphere was attached to a translation stage controlled by a piezoelectric actuator. We used the second harmonic of a continuous wave Nd^{3+} YAG (yttrium aluminum garnet) laser with a linewidth of 1 kHz as the light source. The laser frequency was tuned thermally using the cavity length control and the mode-hop-free tuning range was over 10 GHz. Nearly Gaussian shaped transformed limited pulses were prepared using an electro-optical (EO) modulator with a repetition rate of 100 kHz. We have an option to operate the laser in a continuous wave (cw) mode by applying an electrical bias to the EO modulator. The pulse duration was $\Delta t_p=58$ ns and the frequency width was $\delta\omega_p/2\pi=10$ MHz. The incident laser power was 1 μW. The pulse profile after propagation through the microsphere-fiber-taper system was observed using a streak camera with a time resolution of 10 ps.

To achieve the critical coupling condition, we first adjusted the sphere position along the waist region of the fiber taper monitoring the transmission intensity to become less than 2–3%. Figure 4(a) shows the steady-state measurement of the transmission intensity as a function of the laser frequency. In this measurement, the EO modulator was operated in the cw mode and the laser frequency was scanned across the resonance. The resonance dip has a frequency width of $\delta\omega/2\pi=35$ MHz. Then, we made fine adjustment of the sphere position to find the critical coupling condition so that the dynamic pulse splitting appeared most clearly. Figure 4(b) shows a two-dimensional contour plot of the pulse intensity as a function of time and frequency detuning of the laser at a critical coupling condition. In this measurement the EO moderator was operated in the pulse mode. The laser detuning frequency was continuously scanned and the transmitted pulse profile was monitored through the streak camera. Figure 4(c) shows the pulse profile along the vertical dashed line shown in Fig. 4(b). The solid thin line shows the experimental result. The pulse profile is split into two peaks temporally and the experiment correctly demonstrates the dynamic pulse splitting. The dotted curve in Fig. 4(c) is the theoretical profile calculated using Eqs. (1) and (2) with $x=0.999903$ and $y=0.999904$, assuming a Gaussian shaped initial pulse. While the experiment and theory are in good agreement in showing the dynamic pulse splitting, some of the details of the experimentally observed transmitted profile differ from the theoretically expected shape; especially, the dip between the two peaks does not drop to zero. At the critical coupling condition, most of the ballistic and circulated pulses are canceled, and the transmission intensity approaches zero. Therefore, the transmitted pulses shape could be very sensitive to the initial pulse shape, such as any asymmetry, or even a small deviation from an ideal Gaussian. In addition, the pulse shape could also be sensitive to the small out-coupling of the circulating light into higher modes of the fiber taper. The circulated pulses coupled back into the fundamental fiber mode interferes with the ballistic pulse and results in the dynamic pulse splitting. On the other hand, the circulated pulse which is out-coupled into the higher fiber mode does not interfere with the ballistic pulse propagating in the fundamental fiber mode, but is added as the intensity profile. The temporal position of the circulated pulse is located between the two peaks, therefore this model explains why the dip between the two peaks does not go to zero around the zero delay time. The thick solid curve in Fig. 4(c) is a theoretically calculated pulse profile that incorporates this leakage by assuming that 2.9% of the circulated light is coupled into higher modes in the fiber. This calculated curve shows good agreement with the observation.

In summary, we have discussed fast and slow light in a microsphere-optical-fiber system in the time domain. Fast and slow light are explained as interference effects between ballistic and circulated light. This explanation gives a clear picture, not only for the undercoupling and overcoupling conditions but also for the critical coupling condition where the conventional definition of phase velocity diverges. Recently, theoretical analysis revealed that the coherent effects of a coupled microresonator are remarkably similar to those in atoms. Experimentally, it was clearly demonstrated that coupled whispering gallery microresonators showed induced transparency and absorption [17,18]. The basic mechanism involved in our single-sphere system could also be an essential and an elementary process in pulse propagation through coupled spheres [13,17,18], serial loop structures [14], and arrays of spheres [13], such as photonic crystals [13,23].

[1] S. Chu and S. Wong, Phys. Rev. Lett. **48**, 738 (1982).
[2] C. Liu, Z. Dutton, C. H. Behroozi, and L. V. Hau, Nature **409**, 490 (2001).
[3] L. J. Wang, A. Kuzmich, and A. Dogariu, Nature **406**, 277 (2000).
[4] A. I. Talukder, T. Haruta, and M. Tomita, Phys. Rev. Lett. **94**, 223901 (2005).
[5] A. M. Steinberg, P. G. Kwiat, and R. Y. Chiao, Phys. Rev. Lett. **71**, 708 (1993).
[6] D. R. Solli, C. F. McCormick, C. Ropers, J. J. Morehead, R. Y. Chiao, and J. M. Hickmann, Phys. Rev. Lett. **91**, 143906 (2003).
[7] Y. A. Vlasov, M. O'Boyle, H. F. Hamann, and S. J. McNab, Nature **438**, 65 (2005).
[8] C. F. Bohren and D. R. Huffman, *Absorption and Scattering of Light by Small Particles* (John Wiley & Sons, New York, 1983).
[9] M. Tomita, K. Totsuka, H. Ikari, K. Ohara, H. Mimura, H. Watanabe, H. Kume, and T. Matsumoto, Appl. Phys. Lett. **89**, 061126 (2006).
[10] A. A. Savchenkov, V. S. Ilchenko, A. B. Matsko, and L. Maleki, Phys. Rev. A **70**, 051804(R) (2004).

[11] K. Totsuka and M. Tomita, Phys. Rev. E **73**, 045602(R) (2006).
[12] K. Totsuka and M. Tomita, J. Opt. Soc. Am. B **23**, 2194 (2006).
[13] Y. Hara, T. Mukaiyama, K. Takeda, and M. Kuwata-Gonokami, Phys. Rev. Lett. **94**, 203905 (2005).
[14] J. K. S. Poon, L. Zhu, G. A. DeRose, and A. Yariv, Opt. Lett. **31**, 456 (2006).
[15] D. S. Wiersma, P. Bartolini, A. Lagendijk, and R. Righini, Nature **390**, 671 (1997).
[16] M. Cai, O. Painter, and K. J. Vahala, Phys. Rev. Lett. **85**, 74 (2000).
[17] D. D. Smith, H. Chang, K. A. Fuller, A. T. Rosenberger, and R. W. Boyd, Phys. Rev. A **69**, 063804 (2004).
[18] A. Naweed, G. Farca, S. I. Shopova, and A. T. Rosenberger, Phys. Rev. A **71**, 043804 (2005).
[19] L. F. Stokes, M. Chodorow, and H. J. Shaw, Opt. Lett. **7**, 288 (1982).
[20] M. D. Crisp, Phys. Rev. A **4**, 2104 (1971).
[21] J. P. Heritage, A. M. Weiner, and R. N. Thurston, Opt. Lett. **10**, 609 (1985).
[22] J. C. Knight, G. Cheung, F. Jacques, and T. A. Birks, Opt. Lett. **22**, 1129 (1997).
[23] E. H. El Boudouti, N. Fettouhi, A. Akjouj, B. Djafari-Rouhani, A. Mir, J. O. Vasseur, L. Dobrzynski, and J. Zemmouri, J. Appl. Phys. **95**, 1102 (2004).